Title: Mapping the plasma proteomic architecture of systemic lupus erythematosus

Geoffrey H. D. Leung[1], Charlotte Bottomley[1], Norzawani Buang[1], Robert T. Maughan[1], Benjamin J. Whittle[1], Boroumand Zeidaabadi[1], Yun-Ju Huang[1,2], Tabitha Turner-Stokes[1,3], Marie Condon[3], Liz Lightstone[1,3], Tom Cairns[3], Marina Botto*[1,3], Matthew C. Pickering*[1,3], James E. Peters *[1,3]

Affiliations:
1. Department of Immunology and Inflammation, Imperial College London, London, UK
2. School of Medicine, Chang Gung University and Division of Rheumatology, Allergy and Immunology, Chang Gung Memorial Hospital, Taoyuan, Taiwan
3. Imperial Lupus Centre, Imperial College Healthcare NHS Trust, London, UK
* co-senior authors

Correspondence to:

James E. Peters
Department of Immunology and Inflammation, Imperial College London, London, UK
E-mail: j.peters@imperial.ac.uk

Summary

Systemic lupus erythematosus (SLE) is a systemic autoimmune disease characterised by autoantibodies to nuclear antigens. SLE is highly heterogeneous, both clinically and immunologically, yet the molecular basis underlying this remains incompletely understood. To address this, we profiled the plasma proteome in 260 SLE patients and 86 healthy volunteers (HVs) using the SomaScan v4.1 platform, quantifying 7,288 analytes corresponding to 6,595 unique proteins. We identified 215 proteins that were robustly differentially abundant between SLE patients and HVs in both discovery (n=207 SLE, n=45 HVs) and validation sets (n=53 SLE, n=41 HVs). Within-cases analyses identified 421 proteins associated with disease activity. Network-based clustering delineated correlated protein modules, including an interferon-associated module and a renal-associated module, each linked to distinct clinical features. Autoantibody-stratified analyses further uncovered distinct proteomic endotypes: anti-Sm positivity was associated with increased interferon-stimulated protein levels (e.g., MX1, ISG15, CXCL10) and reduced circulating small ribonuclear proteins, independent of disease activity. Anti-dsDNA antibodies were associated with elevated levels of CD40 ligand (CD40LG) and the neutrophil protease proteinase-3. Moreover, we identified an association between CD40LG and disease activity specific to the anti-dsDNA positive subgroup. Together, these data define plasma protein signatures of SLE and disease activity, highlight autoantibody-specific molecular phenotypes, and provide a basis for precision medicine.

Graphical abstract

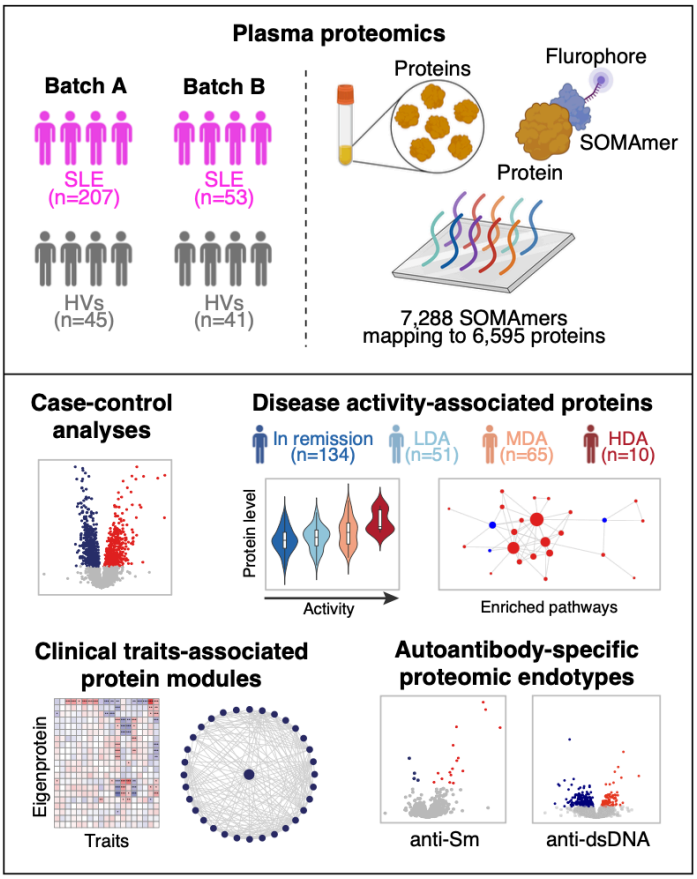

Introduction

Systemic lupus erythematosus (SLE) is an autoimmune disease with complex pathogenesis involving dysregulation of both adaptive and innate immunity. A hallmark of SLE is the production of autoantibodies directed against nuclear antigens (anti-nuclear antibodies; ANA). Established pathogenic pathways include autoreactive B cells, the complement system and type 1 interferon signalling which lead to tissue inflammation and injury. Clinically SLE is highly heterogeneous, ranging from mild to organ- or life-threatening disease, and with variable patterns of organ involvement. There is also inter-patient variability in the targets of ANA. This heterogeneity presents major challenges for patient management, drug development, and trial design. There is a pressing need for a precision medicine approach, matching the right therapy to the right patient. Our ability to deliver such a tailored therapeutic strategy is hampered by insufficient understanding of the molecular basis of heterogeneity and we lack biomarkers that can identify patient subgroups who would benefit from pharmacological targeting of specific pathways.

The advent of genomic technologies has enabled comprehensive assessment of various molecular domains in SLE such as the genome or transcriptome. Genome-wide association studies (GWAS) have elucidated genetic risk factors for SLE [1-3], while transcriptomic studies have revealed the dysregulated gene expression programmes that occur once disease is established [4-6]. A key finding from the latter was the identification of the interferon-stimulated gene (ISG) signature, a gene expression signature indicating stimulation by interferons, particularly type 1 interferons [4, 7-9]. By contrast, few studies have investigated the proteome in SLE [10-12]. Proteins are the effector molecules of biology and the targets of most drugs. In addition, circulating proteins (measurable in plasma or serum) can provide useful and tractable biomarkers suitable for measurement in clinical practice. Thus, evaluation of proteomic changes in SLE could be valuable both for understanding pathogenesis and for translational research [13]. Advances in proteomic technologies now allow for highly multiplexed protein measurements. Here we performed plasma proteomic profiling using the SomaScan platform, measuring 7,288 protein analytes. Our data identify differentially abundant proteins in SLE versus HVs, protein signatures of active disease, and modules of correlated proteins associated with clinical traits. Moreover, we identify auto-antibody specific proteomic endotypes, with distinct proteomic patterns correlated with Smith and dsDNA auto-antibody positivity. These findings provide a basis for precision medicine approaches in SLE.

Results

Plasma proteomic profiles of SLE

We recruited 260 patients with SLE and 86 healthy volunteers (HVs). The cohort encompassed a wide range of disease duration and disease activity (**Table 1**). Seventy patients (28%) had anti-double-stranded DNA (dsDNA) autoantibodies, 193 (75%) anti-Smith (Sm) autoantibodies, and 186 (72%) had anti-ribonucleoprotein (RNP) autoantibodies (**Table 1**). Reduced complement C3 (<0.70 g/L) was observed in 14% of samples and reduced complement C4 (<0.16 g/L) in 26%. One hundred and fifty-eight patients (61%) had a history of previous lupus nephritis (LN) **(Supplementary Data 1)**, but only 10 patients had recent LN (defined as blood sampling within 3 months of a renal biopsy showing LN). Proteomic measurements were performed in two batches. After quality control, 260 SLE and 86 HV samples were available for analysis. Batch A ("discovery set") consisted of 207 SLE samples and 45 HV samples and batch B ("validation set") consisted of 53 SLE samples and 41 HV samples.

To identify proteomic signatures associated with SLE, we performed differential protein abundance testing of SLE versus HVs. For readability, where reporting the number of associations we use the term 'protein' to refer to the protein target of each SOMAmer, but provide further detail of SOMAmer to protein mapping in the Supplementary Data. In Batch A (n=207 SLE, n=45 HVs), we identified 1,821 proteins associated with SLE (1,065 upregulated, 756 downregulated; FDR <0.05) (**Figure 1A**, **Supplementary Figure 1A, Supplementary Data 2**). In batch B (53 SLE, 41 HVs), we identified 428 differentially abundant proteins (268 upregulated, 160 downregulated; FDR <0.05) **(Supplementary Figure 1B, Supplementary Data 3)**. 215 of the 1,821 significant associations from batch A replicated in batch B at FDR <0.05 **(Figure 1A, Supplementary Data 4)**. The estimated effect sizes for these replicated proteins were strongly correlated between the two batches (Pearson's r 0.94) (**Figure 1B**). We then performed a meta-analysis of the two batches to obtain an overall estimate of the effect sizes for the replicated proteins (**Figure 1C. Supplementary Data 4**). Notably, there was marked upregulation of interferon-stimulated proteins (ISPs) in SLE, including ISG15, MX1, STAT1, B2M, DDX58, IFIT3, CXCL11 **(Figure 1D)**. Other strongly upregulated proteins included TNFRSF1B (TNF-R2), VSIG4 (the receptor for complement C3b and iC3b) and the complement fragment C3d. The most downregulated protein was CRISPLD2, a secreted LPS-binding glycoprotein that dampens TLR4-mediated cytokine responses [14]. Gene Set Enrichment Analysis (GSEA) identified 8 pathways that were significantly enriched in both batches, including

70 multiple terms reflecting interferon signalling, as well as SRP-mediated cotranslational protein
71 targeting, and downregulated PI3K/AKT signalling **(Figure 1E, Supplementary Data 5).**
72
73 Plasma proteomic signatures of lupus disease activity
74 Samples were obtained from patients with a range of disease activities; 134 patients were in
75 clinical remission, 51 had low disease activity (LDA), 65 had moderate disease activity (MDA),
76 and 10 had high disease activity (HDA) (definitions in **Methods**). We tested for proteomic
77 associations with SLE disease activity in SLE coded as ordinal variable. To increase power, we
78 analysed both Batch A and B together, adjusting for batch. 421 proteins were significantly
79 associated (FDR <0.05) with disease activity (**Figure 2A, Supplementary Data 6**). As a
80 sensitivity analysis, we performed Spearman's correlation analysis between SLEDAI and each
81 protein, which showed similar results (**Supplementary Figure 2**).
82
83 GSEA revealed significant enrichment of 90 pathways (**Supplementary Data 7**), the most
84 significant of which were "immunoregulatory interactions between a lymphoid and a non-
85 lymphoid cell" and "cytokine-cytokine receptor interaction". The proteins most strongly
86 associated with disease activity by p-value were CD40LG, VIP (vasoactive intestinal peptide)
87 and C1QC (all P_{BH} 1.77×10^{-6}). Active disease was also associated with other complement-
88 related proteins, including increased C3d and VSIG4 and decreased C4 and CFP (properdin)
89 (**Figure 2B**). ISPs (MX1, B2M, CXCL10) were positively associated with disease activity, with
90 MX1 showing the greatest effect size. Levels of type I, II and III interferons were also associated
91 with active disease, with IFNL1 (a type III interferon) showing the strongest effect. Evaluation of
92 connections between IFNL1 and other disease activity-associated proteins revealed IFNL1 was
93 co-correlated (|Pearson's r| >0.6) with 75 other proteins (**Figure 2C, Supplementary Data 8**).
94
95 The SomaScan includes many proteins that are primarily intracellular. Their detection in plasma
96 may reflect cell death and turnover. While such proteins may be useful biomarkers of disease
97 activity, some are likely to be downstream read-outs of tissue inflammation and injury rather
98 than upstream pathogenic drivers. In contrast, plasma proteins associated with disease activity
99 that have a biological role in blood may be more promising therapeutic candidates. For example,
100 cytokines and their receptors have proven to be important therapeutic targets in inflammatory
101 diseases. We therefore extracted a list of proteins annotated in the KEGG 'Cytokine–cytokine
102 receptor interaction' pathway and intersected this with the list of SLE activity-associated proteins
103 (**Figure 2D**). In active SLE, there was upregulation of TNF superfamily and TNF receptor
104 superfamily members (e.g., TNFSF4 (OX40L), TNFSF15 (TL1A), TNFRSF1B (TNFR2),

105 TNFRSF10B (DR5)), chemokines (e.g., CCL2, CCL27, CXCL10, CXCL14), interleukins (e.g.,
106 IL6, IL11, IL24), and growth factors. In contrast, there was downregulation of anti-inflammatory
107 proteins including IL10RA and the decoy receptor IL1R2.
108
109 Associations with complement proteins
110 Given the strong links between complement proteins and disease activity in the literature and in
111 our data, we further analysed proteomic associations with serum complement C3 and C4
112 measured in the clinical laboratory (n=260 SLE patients). Both C3 and C4 were also included
113 on the SomaScan assay. There was very strong concordance of protein measurements between
114 the SomaScan and the clinical laboratory for C4 (ρ 0.95 in Batch A, 0.91 in Batch B), and
115 moderately strong correlation for C3 (ρ 0.61 in Batch A, 0.45 in Batch B) (**Supplementary**
116 **Figures 3A-B**), providing validation of SomaScan measurements. In addition, various
117 complement cleavage fragments were measured; correlations with intact C3 and C4 are
118 presented in **Supplementary Figures 4-5**. Sixty protein targets were correlated with clinical
119 laboratory measured C3 ($|\rho| > 0.3$, FDR < 0.05), **Supplementary Data 9**) including 21
120 associated with disease activity (**Supplementary Figures 6A-B**). Sixty-two proteins were
121 significantly correlated with C4 (**Supplementary Data 10**), 13 of which were disease activity
122 associated (**Supplementary Figure 6C**). In total, 24 protein targets were associated with
123 disease activity and levels of C3 and/or C4 (**Supplementary Figure 6D**). Proteins associated
124 with higher disease activity and lower C3/C4 included CD40LG, interferon-stimulated proteins
125 (e.g. ISG15, IFIT3, LAG3), and C1QC, while IL36A, complement-related proteins (CFP
126 (properdin), FCN1 (ficolin) and C2) and IFNAR1 showed the opposite relationships. The latter
127 may reflect compensatory downregulation in the context of chronic interferon stimulation.
128
129 Exploratory Longitudinal Analysis
130 For 3 patients, longitudinal samples taken at 4 or more timepoints were available. The limited
131 sample size precluded formal biomarker analysis, but we used these data to further explore 7
132 selected proteins (CXCL10, CCL2, CD40LG, HAVCR2, C3d, MX1, B2M) that we had identified
133 as disease activity-associated in the cross-sectional analysis (see **Methods)**. The levels of these
134 proteins generally mirrored disease activity over time, showing positive longitudinal correlations
135 with SLEDAI-2K and anti-dsDNA, and negative correlations with C3/C4 (**Supplementary**
136 **Figures 7A-B**). CD40LG strongly correlated with anti-dsDNA titres, in keeping with its role in B
137 cell activation (**Supplementary Figure 7C**). Longitudinal changes in C3d were inversely
138 correlated with clinically measured C3 (**Supplementary Figure 7D**), in keeping with the known
139 biology of the complement pathway activation whereby cleavage of C3 reduces the amount of

140 intact C3 and increases C3d. Several proteins returned to normal levels (defined based on HV
141 samples) as disease activity declined, though the levels of the ISPs CXCL10, MX1 and B2M
142 failed to fully normalise, suggesting persistent interferon pathway activation (**Supplementary**
143 **Figure 7A)**.
144
145 Network analysis reveals protein modules associated with clinical phenotype
146 We used weighted gene co-expression network analysis (WGCNA) to construct a protein-
147 protein correlation network, identifying 21 protein modules. We then tested for associations
148 between each module and traits including SLEDAI-2K score, ISG score (measured by
149 quantitative polymerase chain reaction, qPCR) and clinical laboratory parameters. The red
150 module, consisting of 35 proteins, was significantly correlated with multiple clinical traits, with
151 positive correlation with SLEDAI-2K score, and multiple autoantibodies, and was negatively
152 correlated with neutrophil and lymphocyte count and levels of haemoglobin, albumin, and
153 complement C3 and C4 (**Figures 3A-E, Supplementary Figures 8A-G**). Notably, this module
154 showed strongest correlation with ISG score (ρ 0.75, P_{BH} 2.4×10^{-29}; **Figure 3B**), and pathway
155 analysis showed enrichment for interferon signalling pathways (**Figure 3F**). ISG15 (measured
156 by SOMAmer seq.14148.2) was the hub protein in this IFN-associated module (**Figure 3G,**
157 **Supplementary Data 11**). ISG15 is an ISP and the module contained other ISPs (including
158 CXCL10, CXCL11, DDX58, MX1, STAT1) and also IFNL1. While red module membership was
159 dominated by interferon-related proteins, the module also contained other proteins including the
160 complement component C1QC, the membrane protein APOL2, and LAG3. These protein
161 network correlations may suggest interplay between C1Q, interferon pathways, and immune
162 signalling. Specifically, LAG3 is a negative regulator of T cell responses, thus suggesting that
163 interferon stimulation (indicated by upregulation of ISPs) may correlate with T cell inhibition.
164
165 The blue module, which had the second-highest number of clinical associations, was positively
166 correlated with creatinine (ρ 0.52, P_{BH} 7.1×10^{-14}) and proteinuria (ρ 0.45, P_{BH} 5.4×10^{-10}) and
167 negatively correlated with albumin **(Figures 3A, 4A-B)**, indicating a link to renal dysfunction.
168 Consistent with this, the module contained Cystatin C (CST3, an accurate marker of glomerular
169 filtration rate; **Figure 4C**), Osteopontin (SPP1, a biomarker of kidney injury), and Parathyroid
170 hormone (PTH which is dysregulated in renal impairment); (**Figures 4C-D, Supplementary**
171 **Data 12**). Other renal-related proteins included Ephrin and Ephrin receptors, which are
172 associated with glomerular podocyte survival, angiogenic modelling and responses to renal
173 injury [15, 16]. Comprising 611 proteins, this renal-associated module was enriched for
174 extracellular matrix-related pathways, possibly reflecting renal scarring (**Figure 4E**). Moreover,

175 the module eigenprotein was significantly higher in patients with a history of LN, particularly
176 those with recent LN, compared with those who never had LN **(Figure 4F)**.
177
178 Autoantibody-specific proteomic endotypes
179 Anti-Sm autoantibodies are highly specific for SLE and are associated with worse prognosis [17,
180 18]. To identify a proteomic signature associated with anti-Sm autoantibodies, we compared the
181 abundance levels of each protein between anti-Sm(+) (n=63) and anti-Sm(-) (n=193) patients.
182 Eighty-three proteins were differentially abundant, with 63 proteins upregulated and 20
183 downregulated in the anti-Sm(+) samples (**Figure 5A**). We considered the possibility that
184 disease activity might be confounded with anti-Sm autoantibody positivity, since patients with
185 Sm antibodies tend to have a worse prognosis and that some of the Sm-associated proteins
186 were associated with disease activity in our previous analyses. We therefore performed multiple
187 linear regression, controlling for disease activity. This revealed 54 proteins associated with anti-
188 Sm antibodies independent of disease activity (43 proteins positively and 11 negatively
189 correlated; **Figure 5B, Supplementary Data 13**). Visualisation of abundance of these proteins
190 against anti-Sm status stratified by disease activity confirmed that the association with Sm
191 antibodies was independent of disease activity (**Figure 5C, Supplementary Figure 9**). Pathway
192 enrichment analysis revealed Sm-associated proteins were enriched for SARS-Cov-2-related,
193 interferon signalling, snRNP assembly, and RNA processing pathway terms (**Figure 5D**). These
194 pathway enrichment terms reflected increases in ISPs and reductions of small nuclear
195 ribonucleoproteins (snRNPs) (**Figure 5E**). ISPs increased in Sm+ SLE included ISG15
196 (SOMAmer seq.14148.2), MX1, CXCL10, GBP1, DDX58, CXCL11, APOL2, STAT1, LGALS9,
197 EPHB2, and LAG3. Since small nuclear ribonucleoproteins (snRNPs) are the targets of anti-Sm
198 antibodies, it is possible that the reduction in circulating snRNPs reflects autoantibody-mediated
199 depletion.
200
201 We then analysed the associations between proteins and anti-dsDNA antibodies. 874 proteins
202 were associated with anti-dsDNA antibody positivity (**Figure 6A**). After adjusting for a modified
203 disease activity score (which excluded dsDNA antibody status), 374 proteins remained
204 associated with dsDNA antibody status (**Figures 6B-C, Supplementary Data 14**). The most
205 upregulated proteins included CD40LG (CD40 ligand), a costimulatory molecule which activates
206 B and T cells and promotes inflammatory responses [19], ARID3A (a DNA-binding protein), IL11,
207 the neutrophil protease proteinase-3 (PRTN3), and RPS7. Proteins reduced in dsDNA antibody
208 positive SLE included CFP, ITGAV|ITGB3 (the vitronectin receptor, an integrin heterodimer),
209 L1CAM, BPIFB1, and C2. Unlike for Sm autoantibody status, the association of ISPs with anti-

210 dsDNA antibody positivity became non-significant after adjustment for disease activity. As a
211 sensitivity analysis, Spearman's rank correlation was performed to test for correlations between
212 the levels of anti-dsDNA autoantibodies (as a continuous trait) and each protein
213 (**Supplementary Figure 10**). In this sensitivity analysis, CD40LG, PRTN3 and ARID3A were
214 again among the strongest associations. Intriguingly, visualisation of CD40LG association with
215 disease activity stratified by antibody status showed this relationship was restricted to the
216 dsDNA antibody positive subgroup (**Figure 6D**; dsDNA+: P 4.2×10^{-3}, beta 0.07; dsDNA-: P 0.52,
217 neta -0.005). Formal interaction analysis confirmed this effect (P 6.7×10^{-5}).
218
219 <u>Comparison with anifrolumab-induced proteomic changes in TULIP-1 trial</u>
220 Given the prominence of interferon pathways in proteomic signatures in our data, we examined
221 to what extent these signatures might be reversible with anti-type 1 interferon receptor therapy
222 through comparison with an external dataset from the study of Baker et al which analysed 169
223 proteins in SLE pre- and post-anifrolumab in the TULIP-1 trial [20] using Olink and Simoa
224 immunoassays. 158 of these proteins were measured in our SomaScan dataset (reflecting 228
225 SOMAmers since some proteins were measured by multiple SOMAmers). Across these 158
226 proteins, $\log_2$ fold changes from our SLE vs HV comparison were negatively correlated with
227 anifrolumab-vs-placebo changes at week 52 in TULIP-1; (r -0.43; **Supplementary Figure 11A**).
228 Similarly, protein associations with disease activity in our study were inversely correlated with
229 changes following anifrolumab treatment (r -0.52; **Supplementary Figure 11B**). Of the proteins
230 measured in both studies, 30 were associated with disease activity in our study, with 13
231 significantly modulated by anifrolumab treatment. These data underscore the centrality of the
232 interferon response in plasma proteomic signatures of SLE. However, some disease activity-
233 associated proteins were not modulated by anifrolumab, including CD40LG, indicating
234 interferon-independent disease-activity related pathways (**Supplementary Figure 11C**).
235
236 **Discussion**
237
238 We performed wide-angled proteomic profiling in lupus, measuring 7,288 analytes reflecting
239 6,595 unique proteins, representing the most comprehensive assessment of the plasma
240 proteome to date. Proteins differentially abundant in SLE vs healthy volunteers and proteins
241 associated with disease activity reflected known pathogenic pathways in SLE, including
242 dysregulation of adaptive immunity, complement pathways, interferon and TLR signalling,
243 validating the utility of plasma proteomics in uncovering underlying disease mechanisms.

Notably, there was strong upregulation of protein products of the ISG signature in SLE and this was more pronounced in active disease. The lupus ISG was first described in transcriptomic microarray studies of immune cells (whole blood or PBMCs) [4, 7, 21]. Here, we demonstrate that a similar 'ISP' signature is present at the protein level in the extracellular space in blood. Few broad-capture plasma proteomic studies have been conducted in SLE. One prior study used an earlier SomaScan version (1,129 proteins) identified 4 interferon-stimulated proteins (EPHB2, LAG3, CXCL13, and CXCL10) associated with SLE[10]. In our study, all of these proteins were significantly upregulated in SLE samples and with increasing disease activity, validating previous findings. A high ISG is associated with worse prognosis [9], but has not entered clinical practice. A plasma-based ISP rather than a gene expression assay might prove more tractable for clinical translation.

Among the most upregulated interferon-stimulated proteins in the present study were ISG15, MX1, STAT1, CXCL11, B2M and LAG3. LAG3 is an inhibitory receptor expressed on activated T cells. Its expression is increased in the context of chronic antigen exposure (e.g. cancer and chronic viral infection) and leads to T cell exhaustion [22-24]. This may represent a compensatory mechanism to limit immune-mediated tissue damage. Our comparison to proteomic data from the TULIP-1 trial showed that LAG3 was downregulated by anifrolumab. In addition to an interferon-driven ISP, we also directly observed upregulation of interferon proteins themselves. Notably, IFNL1, a type III interferon, was strongly upregulated in both comparison to HVs and the analysis of disease activity. IFNL has received less attention than type 1 interferons in lupus pathogenesis, but its upregulation in SLE has been previously reported [25-29].

Our SomaScan results recapitulated historical studies of the complement pathway proteins beyond intact C3 and C4 (which are currently used in clinical practice as biomarkers) [30]. We observed positive association of C3d and negative association of CFP (properdin) with active disease, in keeping with previous reports [31-34]. C1Qc was one of the most strongly associated proteins with active disease. A previous study reported that C1Q negatively regulates type 1 IFN production by promoting preferential binding of immune complexes (ICs) to monocytes and thus reducing IC activation of pDCs, which are a major producer of type 1 IFNs [35]. However, we observed a strong positive correlation between C1Qc and levels of ISPs. Our data are consistent with the observation of reductions in whole-blood *C1Qc* gene expression following anifrolumab therapy [20].

Disease activity-associated proteins included several members of the TNF superfamily cytokines and receptors. One example was TNFSF4 (OX40L), whose plasma levels increased in more active disease. The *TNFSF4* gene locus is a susceptibility locus for SLE, pointing to its causal role in SLE aetiology [36]. In keeping with this, conditional knock out of B cell OX40L ameliorates mouse models of SLE [37]. Our data add to these lines of evidence suggesting that OX40L is a potential therapeutic target in SLE. Another example was TNFSF15 (TL1A), which is a promising therapeutic target in inflammatory bowel disease [38]. Upregulated TNFSF receptors included TNFRSF1B (TNF-R2), which acts a receptor for both TNF and lymphotoxin alpha (LTA), and TNFRSF10B, the receptor for the apoptosis-inducing cytokines TRAIL. Interleukins increased in active disease included IL6, IL11 and IL24. Conversely, there were negative correlations between disease activity and the anti-inflammatory proteins IL1R2 and IL10RA. IL1R2 is a decoy receptor for IL-1, and reduced IL1R2 would be expected to increase pro-inflammatory IL-1 signalling. IL10RA is a receptor for IL-10, an important anti-inflammatory cytokine. Genetic variants in the *IL10RA* gene are associated with early-onset inflammatory bowel disease [39]. Our findings raise the possibility that insufficient activation of homeostatic mechanisms contribute to increased disease activity, although since our data are observational, we cannot exclude the possibility that reductions in anti-inflammatory proteins are secondary to active disease rather than contributors to it.

Co-expression network analysis identified modules of correlated proteins. Two modules had notable associations with clinical and laboratory parameters. One module correlated with the ISG and multiple autoantibodies, consistent with previous reports linking high ISG expression to autoantibodies to Ro, U1-RNP, Sm, and dsDNA [40, 41]. Its hub protein, ISG15, bridges the type 1 and type 2 interferon pathways: induced by type I interferons, it provides negative feedback to downregulate type I responses while promoting interferon-γ [42]. A previous study identified ISG15-secreting plasmablasts and plasma cells in active SLE [43]. The second protein module reflected renal function and other renal-related physiology, and was enriched for ECM- and fibrosis-related pathways, suggesting it captures renal scarring.

Serological profiles in SLE correlate with clinical phenotype and prognosis [17, 18]. For example, anti-dsDNA antibodies are associated with renal disease and anti-Sm antibodies with poor prognosis. Here we show distinct proteomic signatures associated with anti-Sm and anti-dsDNA antibodies that persist after adjustment for the potential confounder of disease activity. Anti-Sm positive SLE showed increased ISPs and reduced circulating snRNPs, possibly reflecting

314 depletion by anti-Sm antibodies targeting epitopes on small nuclear ribonucleoprotein
315 complexes. Although the reductions in snRNPs were in plasma, this may proxy intracellular
316 abundance, raising questions about anti-Sm effects on cellular machinery. Anti-dsDNA positive
317 SLE was associated with elevation of the neutrophil protease, proteinase-3 (PRTN3). This might
318 reflect release of neutrophil contents via neutrophil extracellular traps (NETs), which are a well-
319 established source of nuclear autoantigens in SLE. It is also possible that anti-dsDNA antibodies
320 drive further NET formation and release of proteinase-3.
321
322 CD40LG showed strong associations across multiple analyses, including correlations with
323 disease activity, dsDNA antibody status, and complement C3/C4 levels. Intriguingly, the
324 association with disease activity was specific to individuals with dsDNA antibodies.
325 CD40LG/CD40 interaction drives B cell differentiation into immunoglobulin (Ig)G-secreting
326 plasma cells, making it central to antibody responses. This is consistent with the associations
327 with dsDNA antibodies (both positivity and titre) and reductions in complement C3/C4 (reflecting
328 complement consumption by immune complexes). Previous studies have identified increased
329 expression of CD40 or CD40LG in immune cells and serum in a range of immune-mediated
330 diseases, including SLE [44], and, in line with our data, Goules et al found that CD40LG was
331 elevated in the sera of SLE patients and associated with dsDNA positivity and disease activity
332 [45]. Further support for a pathogenic role for the CD40 pathway in SLE comes from animal
333 models; blocking the CD40-CD40LG interaction ameliorates lupus-like disease in NZB/SWR or
334 NZB/NZW F1 mice [46, 47] and also reduced dsDNA antibodies. There have been efforts to
335 therapeutically target CD40LG in SLE and other autoimmune diseases. While first generation
336 anti-CD40LG monoclonal antibodies (mAbs) were abandoned due to thrombotic events [48],
337 direct targeting of CD40 or newer generation anti-CD40LG mAbs bioengineered with inert or
338 absent Fc tails circumvents this issue. A phase 2 trial of the anti-CD40 mAb BI655064 in lupus
339 nephritis failed to meet its primary end-point, although post-hoc analysis suggested potential
340 benefits of higher doses [49]. Evaluation of Frexalimab, a bioengineered anti-CD40LG mAb is
341 ongoing (NCT05039840). Notably, comparison of our data to proteomic data from the TULIP-1
342 study revealed that, unlike many of the proteins we found associated with disease activity,
343 CD40LG was unaffected by anifrolumab. This suggests that CD40LG axis inhibition might be a
344 complementary approach to anti-IFN therapy by tackling an orthogonal pathogenic pathway.
345 Given the strong associations between CD40LG and dsDNA Ab and complement levels, our
346 data highlight that a stratified medicine approach for anti-CD40 pathway therapeutics might be
347 beneficial. This concept has parallels to the path to approval of belimumab, which proved

348 effective in SLE when used in serologically defined subsets of patients after initial trial failure
349 [50].
350
351 Our study had several limitations. Although our data were split into a discovery and replication
352 subcohorts for case versus control analysis, this was a single-centre study. For within-cases
353 analyses, we analysed both subcohorts together to boost power and thus we did not have a
354 hold-out set for validation. Patients were sampled opportunistically at various points in the
355 disease course and not at pre-defined timepoints; while this enabled cross-sectional evaluation
356 of markers of disease activity, disease duration, chronic damage and past and current treatment
357 were potential confounders. We did not have sufficient longitudinal samples to formally and
358 systematically evaluate intra-individual changes in disease activity-related markers over time.
359 Future studies using inception cohorts with serial sampling are needed to validate putative
360 biomarkers of disease activity identified in the present study. Finally, interpretation of plasma
361 proteomic measurements can be challenging. In addition to canonical soluble proteins, the
362 SomaScan platform includes targets measuring intracellular and membrane-bound proteins.
363 Their detection may represent release from dead cells. Moreover, where proteins exist in both
364 membrane-bound and cleaved states, it is not always clear whether plasma proteomic assays
365 are exclusively capturing the soluble form or also protein from cell membranes (for example,
366 arising from in vivo sources such as exosomes or from sample handling). Complementary
367 cytometry data on paired samples would provide additional insights.
368
369 In summary, this study provides the most comprehensive map of the plasma proteome in SLE
370 to date. Stratification by autoantibody status reveals distinct proteomic endotypes even after
371 adjustment for disease activity. Our data provide insights into pathogenesis and highlight
372 potential therapeutic targets.

		SLE	Healthy	P value
N, Samples [%]		260	86	
	Female	229 [88.1%]	58 [67.4%]	<0.0001
	Male	31 [11.9%]	28 [32.6%]	
Median age, Years [IQR]		43.9 [34.8, 55.4]	39.5 [30.0, 49.1]	0.001
	Female	44.0 [34.6, 55.5]	39.6 [30.3, 48.1]	0.002
	Male	39.9 [35.3, 51.9]	39.4 [30.6, 50.4]	0.271
N, Disease Activity [%]		260	-	
	In remission	134 [51.5%]	-	
	Low	51 [19.6%]	-	
	Moderate	65 [25%]	-	
	High	10 [3.8%]	-	
Median disease duration, Years [IQR]		12.0 [5.5, 19.6]	-	
N, Lupus nephritis [%]				
	Never	92 [35.4%]		
	Previous	158 [60.8%]	-	
	Recent*	10 [3.8%]	-	
Laboratory parameters				
	C3 level (g/L, Median [IQR])†	1.03 [0.85, 1.20]	-	
	N, Low C3 (<0.7g/L) [%]	36 [13.8%]	-	
	C4 level (g/L, Median [IQR])†	0.21 [0.15, 0.28]	-	
	N, Low C4 (<0.16g/L) [%]	68 [26.2%]	-	
	N, Anti-Sm status‡ [%]	256	-	
	Negative	193 [75.4%]	-	
	Positive	63 [24.6%]	-	
	N, Anti-RNP status [%]	260	-	
	Negative	186 [71.5%]	-	
	Positive	74 [28.5%]	-	
	N, Anti-dsDNA status†‡ [%]	250	-	
	Negative (0-9 IUperML)	140 [56%]	-	
	Borderline (10-20 IUperML)	40 [16%]	-	
	Positive (>20 IUperML)	70 [28%]	-	

Table 1. Characteristics of study participants.
P-value for differences in sex distribution was calculated using chi-squared test; P-values for differences in age were calculated using Student's t-test. *Recent nephritis defined as blood sample taken within 3 months of a renal biopsy showing lupus nephritis. †Anti-dsDNA antibodies and complement levels measured at the time of research sample. ‡Differences in N reflect individuals with missing data for autoantibody status.

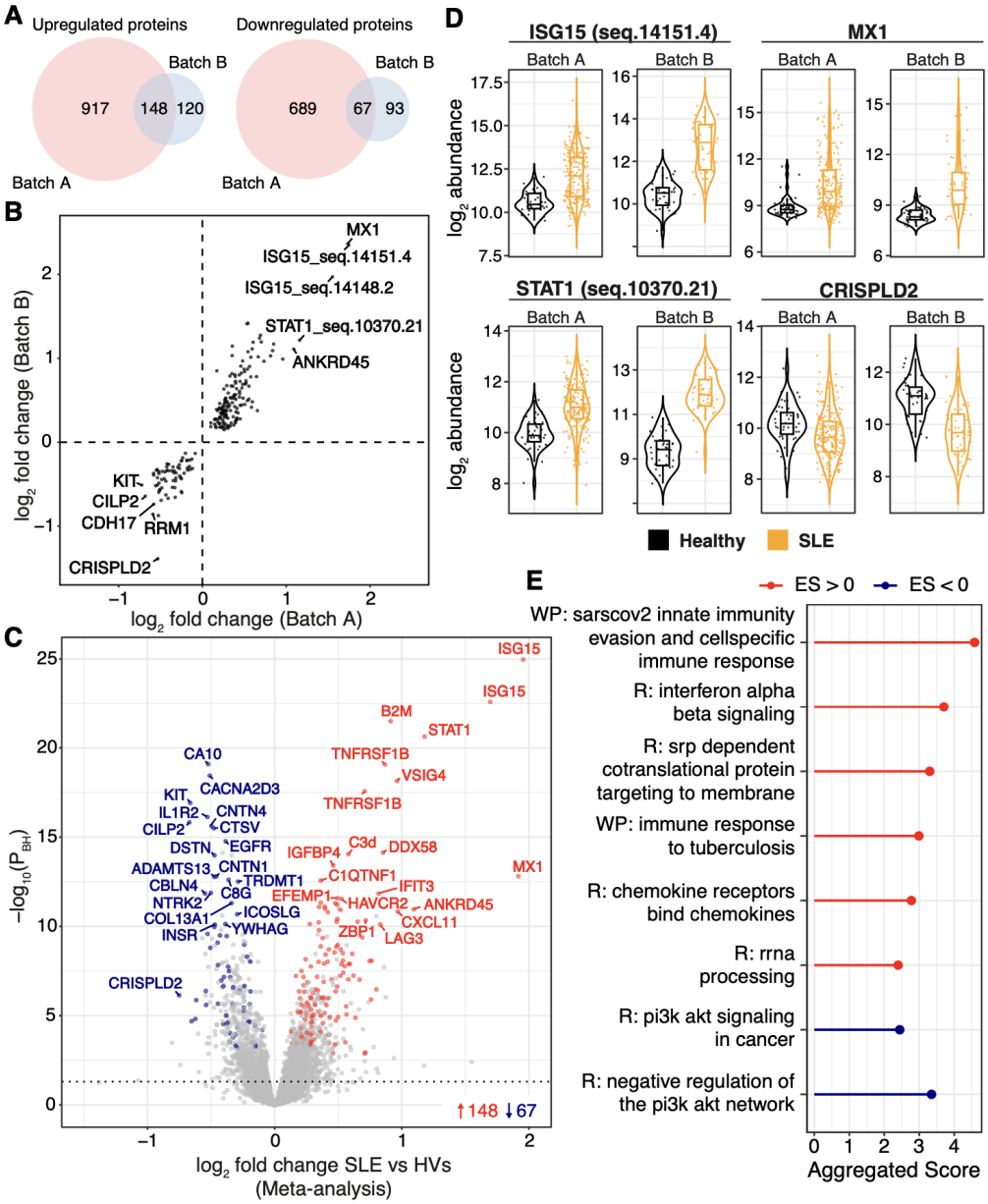

Figure 1. Differentially abundant proteins and enriched pathways in SLE versus healthy volunteers.

A) Venn diagrams of the number of significantly (FDR <0.05) upregulated (left) and downregulated (right) proteins in SLE versus HVs in batch A (n=207 SLE, n=45 HVs) and B (n=53 SLE, n=41 HVs) data. **B)** Comparison of effect size estimates (covariate-adjusted $\log_2$ fold change) for validated proteins between Batch A and Batch B. Each point represents the protein target of a SOMAmer. 215 protein targets which were significantly differentially abundant (FDR <0.05) in both batch A and batch B are shown. The top 5 upregulated and downregulated protein targets (ranked by meta-analysed effect sizes) are annotated. **C)** Volcano plot showing the results from meta-analysis of Batches A and B. Coloured points represent protein targets replicated in both batches (FDR <0.05). Red: upregulated, blue: downregulated, grey: not replicated or non-significant. **D)** Examples of most significant differentially abundant proteins. Each point represents a sample. Orange: SLE, Black: HVs. **E)** Pathways enriched (FDR <0.05) in both batches. Aggregated score was calculated using robust rank aggregation. Red: upregulated pathways. Blue: downregulated pathways. R, Reactome; WP, WikiPathways; ES, Effect size.

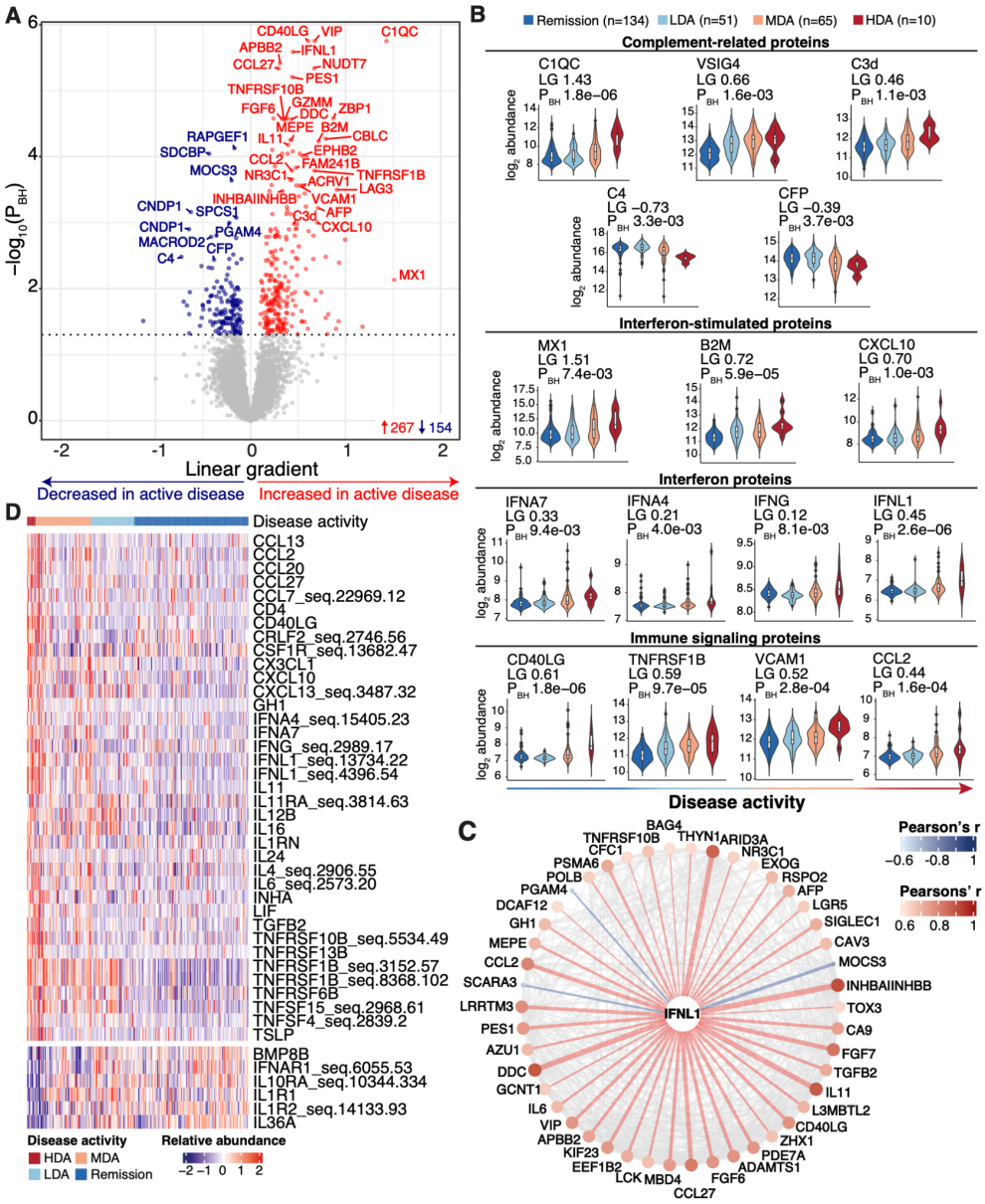

Figure 2. Proteins associated with SLE disease activity.
n=260 SLE samples. **A)** Volcano plot. P_{BH} Benjamini-Hochberg-adjusted P-value (linear regression). Linear gradient shows the magnitude and direction of change in the protein level with increasing disease activity. Dotted line = 5% FDR. Each point represents a protein. Red: significant positive association with active disease, blue: negative association, grey: non-significant. **B)** Examples of disease-associated complement-related, interferon-pathway and immune signalling proteins. LG = Linear gradient. Unique SOMAmer identifiers for displayed proteins where the SomaScan has >1 SOMAmer are: B2M (seq.3485.28), IFNA4 (seq.15405.23), IFNG (seq.2989.17), TNFRSF1B (seq.3152.57), and VCAM1 (seq.2967.8). **C)** Disease activity-associated proteins correlated with IFNL1. For clarity of visualisation, only the proteins associated with disease activity at 1% FDR are displayed. A detailed list of proteins correlated with IFNL1 is provided in Supplementary Data 8. Edges represent pairwise protein correlations with |Pearson's r|>0.6. Node size, colour, and edge thickness indicate the strength of correlation (Pearson's r) with IFNL1. Edge colour denotes correlation direction: blue for negative and red for positive. **D)** Heatmap of significant (FDR <0.05) disease activity-associated proteins in the KEGG Cytokine-Cytokine Receptor Interaction pathway. Protein levels were adjusted for sex and batch.

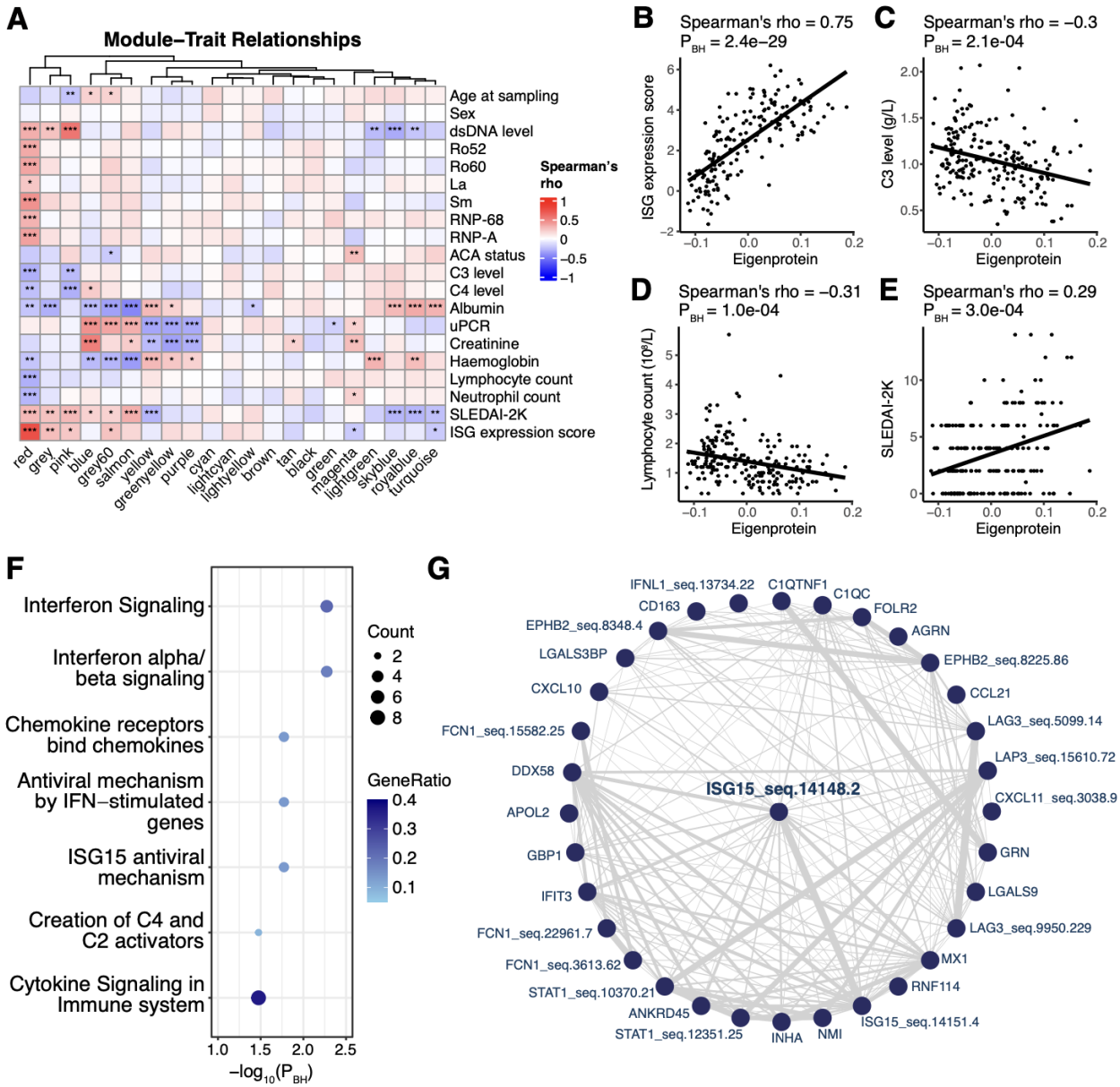

Figure 3. Network analysis identifies protein modules correlated with clinical traits. **A)** Network constructed using SLE samples (n=207). Correlation between each module and clinical traits. Asterixes represent BH-adjusted P values: * < 0.05, ** < 0.01, ***< 0.001. Colour gradient represents Spearman's ρ. **B-E)** Relationships between the eigenprotein values of the red module and clinical traits: **(B)** ISG expression score, **(C)** C3 level, **(D)** lymphocyte count, **(E)** SLEDAI-2K. Each point represents a sample. Solid line indicates best fit from linear regression. **F)** Pathways enriched for proteins in the red module. **G)** Network of protein members of the red module. Edges represent the strength of similarity between each pair of proteins. ISG15 (measured by SOMAmer seq.14148.2) was the module hub protein.

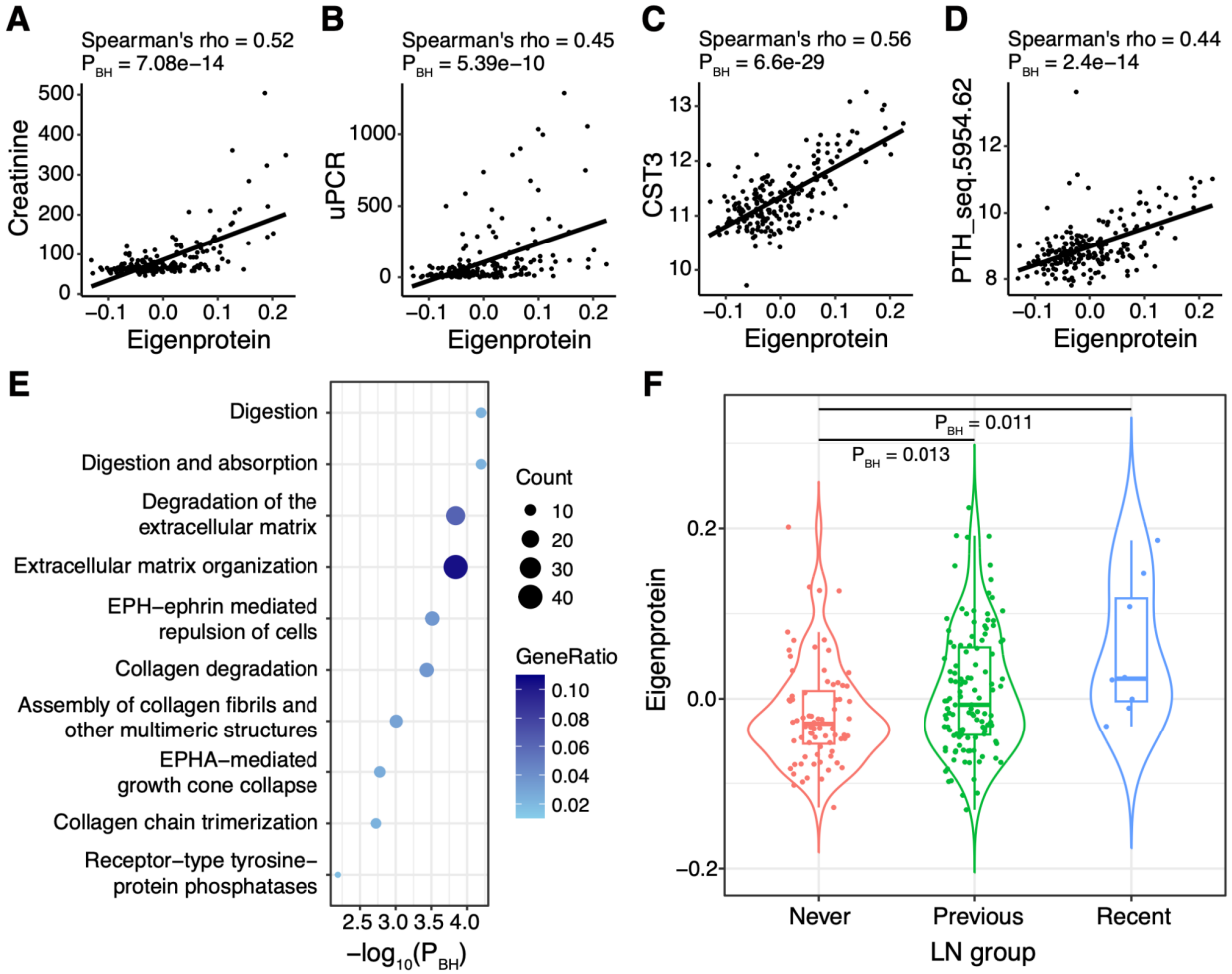

Figure 4. Renal-associated protein module.
A-D) Relationships between the eigenprotein values of the blue module and renal markers: **(A)** Creatinine, **(B)** uPCR, **(C)** cystatin C (CST3), **(D)** parathyroid hormone (PTH). Each point represents an SLE sample. Solid line represents the line of best fit from linear regression. **E)** Pathways enriched for proteins involved in the blue module. **F)** Eigenprotein values of the blue module according to lupus nephritis (LN) status. n=207 SLE samples.

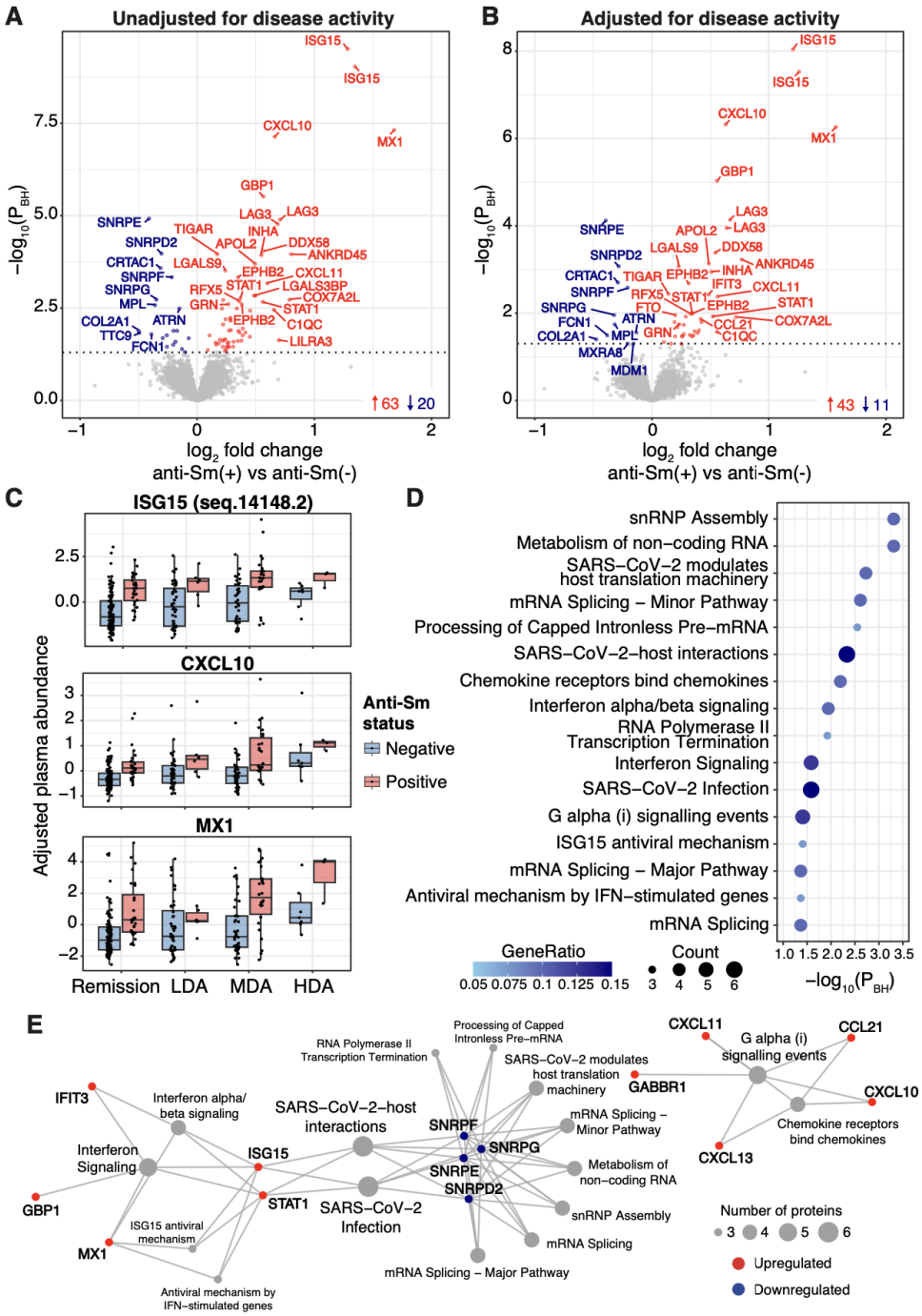

Figure 5. Proteins associated with anti-Sm autoantibodies.
A) Proteins differentially abundant in anti-Sm positive (n=63) versus anti-Sm negative SLE (n=193), without adjustment for disease activity. Each point represents a protein. Red: significantly upregulated, blue: significantly downregulated, grey: non-significant. **B)** As for **A,** but after adjustment for disease activity. **C)** Interferon-stimulated proteins are associated with Sm antibodies independent of disease activity. Displayed protein levels have been adjusted for batch and sex. **D)** Significantly enriched pathways for proteins associated with anti-Sm antibodies after adjustment for disease activity. **E)** Connections between proteins associated with anti-Sm antibodies status independent of disease activity and the enriched pathways. Node size (for pathway terms) represents the number of proteins associated with the pathway. Red: upregulated proteins. Blue: downregulated proteins.

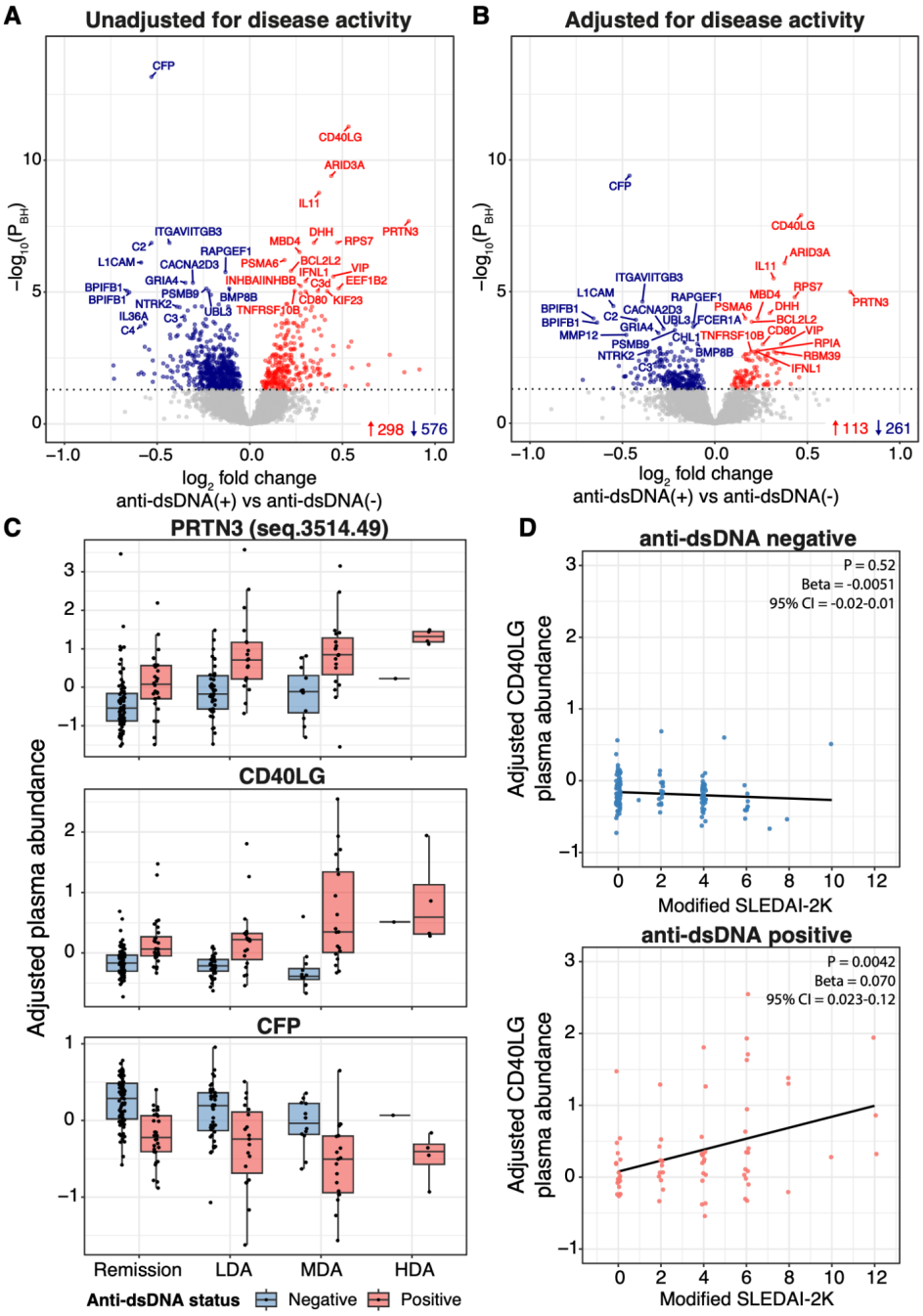

Figure 6. Proteins associated with anti-dsDNA autoantibodies.
A) Proteins differentially abundant in anti-dsDNA positive (n=70) and anti-dsDNA negative (n=140) SLE samples, without adjustment for disease activity. Each point represents a protein. Red: significantly upregulated, blue: significantly downregulated, grey: non-significant. **B)** As for **A**, but after adjustment for disease activity. **C)** Examples of proteins associated with anti-dsDNA antibodies independent of disease activity. Protein levels in ant-dsDNA antibody positive and negative samples are shown stratified by disease activity. **D)** The association of plasma CD40LG with disease activity is restricted to anti-dsDNA positive individuals. SLEDAI-2K modified to exclude anti-dsDNA status from the score. Each point represents an SLE sample. Solid line represents the line of best fit from linear regression. Protein levels in **C** and **D** have been adjusted for batch and sex.

Methods

Subjects and Samples

We recruited 268 patients with SLE from the Imperial Lupus Centre at the Hammersmith Hospital, London, United Kingdom (UK). All patients were anti-nuclear antibody positive and fulfilled the 1997 American College of Rheumatology criteria. We recruited 86 healthy volunteers (HVs) to provide a control group, sampled as two temporally distinct groups comprising 45 and 41 individuals, respectively. No patients had received anifrolumab since this drug is not licensed in the UK.

Human samples used in this research project were obtained from the Imperial College Healthcare Tissue and Biobank (ICHTB). ICHTB is supported by the National Institute for Health Research Biomedical Research Centre based at Imperial College Healthcare NHS Trust and Imperial College London. ICHTB is approved by Wales REC3 to release human material for research (22/WA/0214). Ethical approval was provided by the ICHTB (Human Tissue Authority Licensing number 12275; Project number R14042-3A; sub-collection IMM_MB_13_001) and informed consent obtained from all participants. Peripheral blood was collected in EDTA tubes and centrifuged at 1,000G for 10 minutes at room temperature within three hours of venepuncture and stored at -70°C without freeze-thaw before assay processing.

Proteomic measurements and quality assessment

Plasma proteins were measured using the aptamer-based SomaScan v4.1 platform (Boulder, Colorado, USA). The SomaScan v4.1 platform uses modified aptamers (SOMAmers) that bind to their targeting proteins for measurement. A total of 7,288 SOMAmers targeting 6,595 unique human proteins were measured (some proteins were assayed by multiple distinct SOMAmers; **Supplementary Data 15**). To avoid interference of anti-dsDNA autoantibodies with the SOMAmers, a validated anti-DNA antibody protocol was used [10]. This involved adding herring sperm DNA to saturate anti-dsDNA autoantibodies within each sample and prevent these antibodies from binding the SOMAmers. The platform contains buffer replicates containing no protein which are used to estimate the background noise level, calibrator replicates to control for intra-plate variations and batch effects across experiments, and quality control (QC) replicates for signal normalisation and QC check. Multiple normalisation and calibration steps were performed using SomaLogic's standard protocol. Data normalised by adaptive normalisation by maximum likelihood was used for our analyses. Relative fluorescence units were $\log_2$-transformed before analyses. Proteomic measurements were performed in two separate batches: batch A consisted of 226 SLE and 45 healthy samples and batch B of 57 SLE and 41 HV samples.

In addition to the manufacturer's quality assessment, we performed additional steps including PCA and inspection of sample distributions via boxplots. We identified batch effects, with separation of Batch A and Batch B on PCA. **(Supplementary Figures 12A-B)**. After manual examination on the PCA plot, three samples from Batch A were removed since they were distinctly distributed from the main cohort of samples (>3 standard deviations from the means of PC1 and PC2) and also processed on the same day, suggesting technical rather than biological variation (**Supplementary Figure 12A**). Additionally, 1 sample from batch A and 4 samples from batch B were removed since they were flagged as potential poor quality samples by SomaScan's standard QC pipeline requiring extremely high (>2.5) or low (<0.4) scaling factors for normalisation. For 3 patients, serial longitudinal samples were available. In these instances, we retained the first sample for each patient and excluded the others from all downstream analyses except for the evaluation of intra-individual changes over time in disease activity-associated markers (see below). For the main analyses

(excluding serial samples), post QC samples sizes were as follows: Batch A: 207 SLE, 45 HVs and Batch B: 53 SLE, 41 HVs.

Protein nomenclature

Due to non-standardisation of protein nomenclature (e.g. where a given protein has multiple names) and the lack of human-interpretability of Uniprot identifiers, we annotated each protein using the non-italicised gene HUGO symbol of the encoding gene. In instances where there were multiple distinct SOMAmers mapping to the same HUGO gene symbol (1,669 SOMAmers mapped to 781 unique gene symbols and 782 Uniprot identifiers), we concatenated the gene symbol with the SOMAmer identifier to preserve a unique identifier for each analyte. Importantly, in some instances, multiple SOMAmers mapping to the same gene symbol represented measurements of distinct biological entities. For example, the intact complement C3 protein and its distinct cleavage products such as C3a, C3b, and C3d, all mapped to a single HUGO gene symbol and Uniprot ID. However, in other instances there were multiple SOMAmers that are nominally directed against the same target protein. A comprehensive annotation file mapping of SOMAmers to their target proteins, Uniprot IDs and corresponding gene IDs, and gene symbols is provided in **Supplementary Data 15**.

Complement proteins

Various complement proteins and cleavage fragments were included on the SomaScan platform. To evaluate the accuracy of complement C3 and C4 quantification, we compared the levels of intact complement C3 and C4 proteins measured by SomaScan in SLE patients to their corresponding values measured in the clinical laboratory from the same blood draw. We performed this analysis separately for each batch to avoid variation related to batch.

Identification of differentially abundant proteins in SLE vs healthy samples

For each protein measured, multiple linear regression was used to analyse differences in protein abundance between SLE and HVs samples using the lm() function in R. Age and sex were adjusted for by including them as covariates. The regression model in Wilkinson notation was:

$$P \sim D + age + sex$$

where P was plasma level for a given protein and D was a binary variable disease status (SLE vs healthy).

In Batch B, we observed inflation of test statistics and an unusually high proportion of proteins that were significantly differentially abundant in the comparison of SLE vs HVs (**Supplementary Figures 13-14)**. We also observed marked separation of SLE and HV samples on PC1 (when PCA was performed limiting to Batch B; **Supplementary Figure 15**), with PC1 accounting for 42% of the variance. The most upregulated protein was PGAM1, which has been identified by Somalogic as a marker of pre-analytical variation including time to spin, suggesting that systematic non-biological variation was confounding the differences between SLE and HVs in Batch B (**Supplementary Figure 13)**. We therefore included the first principal component as a covariate to adjust for pre-analytical variation in Batch B (see **Supplementary Note**).

Statistical significance

P-values were adjusted using the Benjamini-Hochberg (BH) method (P_{BH}) to control the false discovery rate (FDR) across multiple tests. We defined statistical significance as $P_{BH} < 0.05$ (i.e. leading to an FDR <0.05) for all analyses in this study.

543 Identification of proteins associated with disease activity
544 Disease activity was assessed using the SLE Disease Activity Index (SLEDAI)-2K [51]. Given that
545 SLEDAI-2K scores have a highly non-normal distribution and can be sensitive to the weightings
546 attributed to specific clinical features, prior to testing for association with proteins, we categorised
547 disease activity into a four level ordinal variable as follows: 'high disease activity' (HDA) was defined
548 as SLEDAI-2K ≥ 10; 'moderate disease activity' (MDA) as SLEDAI-2K between 5 and 9; 'low disease
549 activity' (LDA) as SLEDAI-2K ≤ 4 but not meeting the definition for remission; 'remission' as defined
550 by the Definition of Remission in SLE (DORIS) criteria [52], characterized by clinical components of
551 SLEDAI-2K = 0 (i.e. not including dsDNA antibody or complement status) and a prednisolone dose
552 ≤ 5 mg/day.
553
554 To identify proteins associated with disease activity, we performed multiple linear regression for each
555 protein using the lm() function in R. Protein abundance was regressed on disease activity (coded as
556 an ordinal variable: "In remission", "LDA", "MDA", "HDA"), with sex and batch as covariates. As a
557 sensitivity analysis, Spearman's rank correlation was conducted between protein abundance and
558 SLEDAI-2K scores. Prior to correlation testing, protein abundances were adjusted to account for sex
559 and batch effects using a linear model and the resulting residuals were used in the Spearman's
560 correlation test versus SLEDAI-2K scores.
561
562 Exploratory Longitudinal analysis
563 A subset of disease activity–associated proteins was selected for further investigation in a
564 longitudinal analysis of patients (n=3) with samples taken at four or more timepoints. We first
565 selected proteins that were: (i) potential drug targets, defined as having an associated compound
566 with a characterized mechanism of action in Open Targets (Dataset: "Drug - mechanism of action";
567 data version 25.03), and (ii) were members of the pathways significantly enriched among disease
568 activity–associated proteins. From this list we then selected the 5 proteins with the greatest effect
569 sizes in the ordinal linear regression analysis testing for association with disease activity. These
570 criteria resulted in 5 proteins, one of which was an interferon-stimulated protein (CXCL10). In
571 addition, we added two interferon-stimulated proteins that were significantly associated with disease
572 activity. Repeated measures correlation was used to assess the association between these proteins
573 and clinically measured disease activity traits, accounting for the non-independence of observations
574 due to repeated measurements within the same individuals [53]. This approach is more appropriate
575 than Pearson's correlation, which assumes independent observations.
576
577 Identification of proteins associated with autoantibody status
578 We analysed proteomic associations with the presence of antibodies to Smith (Sm), anti-dsDNA and
579 phospholipids. For each plasma protein, abundance (P) was regressed on antibody status (Ab; a
580 binary variable) with batch and sex included as covariates. The regression model in Wilkinson
581 notation was P ~ Ab + batch + sex. To identify associations with Sm antibodies independent of
582 disease activity, we then repeated the analysis adding disease activity status as a covariate to the
583 model.
584
585 For the dsDNA analysis, samples were classified as anti-dsDNA negative if the level was lower than
586 10 IUperML (the manufacturer's defined threshold) and as anti-dsDNA positive if the patient's
587 plasma anti-dsDNA autoantibodies level was higher than 20 IUperML. Patients with anti-dsDNA
588 levels (n=40) within the borderline range of 10-20 IUperML were excluded in this analysis. To identify
589 proteins associated with anti-dsDNA positivity independent of disease activity, we used a modified

SLEDAI-2K score excluding the anti-dsDNA component from the score to avoid over-adjustment since SLEDAI-2K includes 2 points for dsDNA antibody positivity. We re-calibrated the disease activity category thresholds between LDA, MDA and HDA based on this modified score (DORIS remission definition was unchanged since this does not include anti-dsDNA status). Specifically we normalised the modified SLEDAI-2K by the highest possible score excluding dsDNA antibody positivity (i.e., 105-2 = 103), and applied the same procedure to the unmodified SLEDAI-2K thresholds used to define activity categories described earlier. To illustrate this procedure, an individual positive for anti-dsDNA antibodies with an unmodified SLEDAI-2K score of 11 would have been defined as being in HDA (defined as SLEDAI-2K of 10 or higher) in the earlier analyses. The modified SLEDAI-2K score would be 9. The normalised score would be 9/103=0.087. The new cut-off for HDA would be 10/103=0.097. Thus this individual would be classified as in MDA for the purposes of covariate adjustment in the analysis testing for proteins associated with anti-dsDNA antibodies independent of disease activity.

As a sensitivity analysis, we tested protein abundances against anti-dsDNA titre (as a continuous variable) using all available SLE samples. To do this, protein abundances were first adjusted to account for sex, batch and disease activity (as an ordinal variable) using a linear model and the resulting residuals were used in the Spearman's correlation test versus anti-dsDNA titre.

To formally test whether CD40LG's association with disease activity was dependent on dsDNA antibody status, we fitted a regression model with an dsDNA antibody status as a binary variable (Ab) x disease activity interaction term:

CD40LG ~ Ab + disease_activity + Ab:disease_activity + batch + sex

A significant interaction term indicates that the effect of disease activity on the protein is dependent on dsDNA antibody status.

<u>Pathway enrichment analyses</u>

For SLE-vs-HVs comparisons and disease activity analysis, we performed Gene Set Enrichment Analysis (GSEA) using the fgsea R package (version 1.24.0) [54] and the Human MSigDB Collection "C2: curated gene sets" (sub-collection: "Canonical pathways") which consists of 4,023 gene sets (v2025.1) mainly sourced and curated from BioCarta, Kyoto Encyclopedia of Genes and Genomes, Pathway Interaction Database, Reactome, and WikiPathways [55]. For SLE-vs-HVs comparisons, GSEA was performed separately in each batch. We then used robust-rank aggregation (RRA) [56] to identify the pathways most consistently enriched across both batches. RRA outputs a score analogous to a P-value for each pathway term. These scores were -log10 transformed to represent the aggregated score. A higher aggregated score indicates stronger consistency.

Over-representation tests were used to identify enriched pathways in WGCNA protein modules and antibody-associated protein lists, implemented using the 'enrichPathway' function from the ReactomePA R package (v1.42.0) [57]. Proteins were first mapped to corresponding Entrez IDs since this package requires Entrez ID annotation. Entrez IDs mapped to proteins in the module were tested against the background set of 6,363 Entrez IDs representing the proteins measured on SomaScan v4.1. All pathway enrichment analyses were restricted to protein sets containing 10–500

proteins to exclude very small sets vulnerable to noise and large sets representing broad and non-specific processes.

Protein network analysis

We applied the Weighted Gene Co-expression Network Analysis (WGCNA) package (v1.72-5) [58] to identify modules of correlated proteins. For this analysis we used SLE samples (n=207) from Batch A. A soft thresholding power of 6 was selected based on the criterion of scale-free topology and mean connectivity. Networks were constructed and modules were identified by the adjacency and topology overlap matrices, with minimum module size set to 20. We then refined the modules by their similarity based on modular eigenprotein (representing the first principal component of each module's protein abundance profile) correlation using a dynamic tree-cut approach. Modules were merged if their eigenprotein-based dissimilarity was below a threshold of 0.25. The resulting modular eigenproteins were then used to correlate with 20 clinical traits using Spearman's rank correlation test, including 11 continuous traits: age, SLEDAI-2K, neutrophil count, lymphocyte count, haemoglobin, creatinine, urine protein-creatinine ratio (uPCR), albumin, complement C3, complement C4, and whole-blood ISG score (see below), and 9 binary traits: positivity of antibodies against cardiolipin (ACA), RNP-A, RNP-68, Sm, La, Ro52, Ro60, dsDNA, and sex. Correlations with $P_{BH} < 0.05$ were considered significant. Eigenprotein-based connectivity, or module membership, was calculated for each protein in each module by correlation between the protein abundance levels and the corresponding module's eigenprotein values. The protein with highest module membership was then defined as the hub protein for each module. The network of the proteins in the selected module was constructed using the topology overlap matrix which calculates the strength of similarity between each pair of proteins. The network was then visualised in Cytoscape (v3.10.3) [59], with nodes representing proteins and thickness of edges representing the strength of similarity. Only the edges with a threshold value of > 0.03 were included in the visualised network.

Whole-blood interferon stimulated gene score

The whole-blood interferon-stimulated gene score was measured as described previously [60]. In brief, total RNA was isolated from whole blood samples using Tempus RNA isolation kits (Thermo Fisher Scientific) following the manufacturer's protocol. Gene expression was measured by real-time qPCR and relative gene expression of *CMPK2*, *EPSTI1* and *HERC5* were calculated by subtracting the housekeeping gene *HPRT* using the ΔCt method. The ISG score was calculated using the mean ΔCt from *CMPK2*, *EPSTI1* and *HERC5* genes *(-1).

Resource availability

Lead contact

Requests for further information and resources should be directed to the lead contact, James E. Peters (j.peters@imperial.ac.uk).

Materials availability

This study did not generate new unique reagents.

Declaration of interests

Dr Lightstone reports the following: Advisor / Consultant to: Alexion, Argenx, Astra Zeneca, Boehringer Ingelheim, Carna Health, GSK, Incyte, Kezar, Nkarta, Novartis, Otsuka, Pfizer, Roche, Sanofi, Vera, Vertex; Speaker bureaux: Astra Zeneca, GSK, Otsuka, Roche; Trial data monitoring committees: Nkarta, Novartis. The other authors declare that they have no known competing financial interests or personal relationships that could have appeared to influence the work reported in this paper.

Acknowledgements

The study was funded by a Medical Research Foundation Fellowship to J.E.P. (MRF-057-0003-RG-PETE-C0799) and by the NIHR Imperial Biomedical Research Centre Immunology Theme. The views expressed are those of the authors and not necessarily those of the NIHR or the Department of Health and Social Care. M.C.P. is a Wellcome Trust Senior Fellow in Clinical Science (grant no. 212252/Z/18/Z). We thank Shanice Lewis for technical assistance.

691 **References**
692

693 1. Bentham, J., et al., Genetic association analyses implicate aberrant regulation of innate and
694 adaptive immunity genes in the pathogenesis of systemic lupus erythematosus. *Nat Genet*,
695 2015. **47**(12): p. 1457-1464.
696 2. Langefeld, C.D., et al., Transancestral mapping and genetic load in systemic lupus
697 erythematosus. *Nat Commun*, 2017. **8**: p. 16021.
698 3. Wang, Y.F., et al., Identification of 38 novel loci for systemic lupus erythematosus and genetic
699 heterogeneity between ancestral groups. *Nat Commun*, 2021. **12**(1): p. 772.
700 4. Baechler, E.C., et al., Interferon-inducible gene expression signature in peripheral blood cells
701 of patients with severe lupus. *Proc Natl Acad Sci U S A*, 2003. **100**(5): p. 2610-5.
702 5. Panousis, N.I., et al., Combined genetic and transcriptome analysis of patients with SLE:
703 distinct, targetable signatures for susceptibility and severity. *Ann Rheum Dis*, 2019. **78**(8): p.
704 1079-1089.
705 6. Nakano, M., et al., Distinct transcriptome architectures underlying lupus establishment and
706 exacerbation. *Cell*, 2022. **185**(18): p. 3375-3389 e21.
707 7. Bennett, L., et al., Interferon and granulopoiesis signatures in systemic lupus erythematosus
708 blood. *J Exp Med*, 2003. **197**(6): p. 711-23.
709 8. Postal, M., et al., Type I interferon in the pathogenesis of systemic lupus erythematosus. *Curr*
710 *Opin Immunol*, 2020. **67**: p. 87-94.
711 9. Psarras, A., M. Wittmann, and E.M. Vital, Emerging concepts of type I interferons in SLE
712 pathogenesis and therapy. *Nat Rev Rheumatol*, 2022. **18**(10): p. 575-590.
713 10. Smith, M.A., et al., Using the circulating proteome to assess type I interferon activity in
714 systemic lupus erythematosus. *Sci Rep*, 2020. **10**(1): p. 4462.
715 11. Su, K.Y.C., et al., Proteomic analysis identifies subgroups of patients with active systemic
716 lupus erythematosus. *Clin Proteomics*, 2023. **20**(1): p. 29.
717 12. Li, Y., et al., Combined proteomics and single cell RNA-sequencing analysis to identify
718 biomarkers of disease diagnosis and disease exacerbation for systemic lupus
719 erythematosus. *Front Immunol*, 2022. **13**: p. 969509.
720 13. Piga, M. and L. Arnaud, The Main Challenges in Systemic Lupus Erythematosus: Where Do
721 We Stand? *J Clin Med*, 2021. **10**(2).
722 14. Wang, Z.Q., et al., The novel lipopolysaccharide-binding protein CRISPLD2 is a critical
723 serum protein to regulate endotoxin function. *J Immunol*, 2009. **183**(10): p. 6646-56.
724 15. Weiss, A.C. and A. Kispert, Eph/ephrin signaling in the kidney and lower urinary tract. *Pediatr*
725 *Nephrol*, 2016. **31**(3): p. 359-71.
726 16. Huang, Z., et al., Key role for EphB2 receptor in kidney fibrosis. *Clin Sci (Lond)*, 2021.
727 **135**(17): p. 2127-2142.
728 17. Gomez, A., et al., Treat-to-target in SLE: is serology important? Results from an integrated
729 analysis of five randomized clinical trials of belimumab. *Rheumatology (Oxford)*, 2025. **64**(6):
730 p. 3598-3605.
731 18. Arroyo-Avila, M., et al., Clinical associations of anti-Smith antibodies in PROFILE: a multi-
732 ethnic lupus cohort. *Clin Rheumatol*, 2015. **34**(7): p. 1217-23.
733 19. Elgueta, R., et al., Molecular mechanism and function of CD40/CD40L engagement in the
734 immune system. *Immunol Rev*, 2009. **229**(1): p. 152-72.
735 20. Baker, T., et al., Type I interferon blockade with anifrolumab in patients with systemic lupus
736 erythematosus modulates key immunopathological pathways in a gene expression and
737 proteomic analysis of two phase 3 trials. *Ann Rheum Dis*, 2024. **83**(8): p. 1018-1027.
738 21. Han, G.M., et al., Analysis of gene expression profiles in human systemic lupus
739 erythematosus using oligonucleotide microarray. *Genes Immun*, 2003. **4**(3): p. 177-86.
740 22. Ruffo, E., et al., Lymphocyte-activation gene 3 (LAG3): The next immune checkpoint
741 receptor. *Semin Immunol*, 2019. **42**: p. 101305.
742 23. Andrews, L.P., et al., LAG-3 and PD-1 synergize on CD8(+) T cells to drive T cell exhaustion
743 and hinder autocrine IFN-gamma-dependent anti-tumor immunity. *Cell*, 2024. **187**(16): p.
744 4355-4372 e22.

745 24. Gao, Z., et al., T-cell exhaustion in immune-mediated inflammatory diseases: New
746 implications for immunotherapy. *Front Immunol*, 2022. **13**: p. 977394.
747 25. Wu, Q., et al., Interferon-lambda1 induces peripheral blood mononuclear cell-derived
748 chemokines secretion in patients with systemic lupus erythematosus: its correlation with
749 disease activity. *Arthritis Res Ther*, 2011. **13**(3): p. R88.
750 26. Oke, V., et al., IFN-lambda1 with Th17 axis cytokines and IFN-alpha define different subsets
751 in systemic lupus erythematosus (SLE). *Arthritis Res Ther*, 2017. **19**(1): p. 139.
752 27. Amezcua-Guerra, L.M., et al., Type III Interferons in Systemic Lupus Erythematosus:
753 Association Between Interferon lambda3, Disease Activity, and Anti-Ro/SSA Antibodies. *J*
754 *Clin Rheumatol*, 2017. **23**(7): p. 368-375.
755 28. Chen, J.Y., et al., Interferon-lambda3/4 genetic variants and interferon-lambda3 serum levels
756 are biomarkers of lupus nephritis and disease activity in Taiwanese. *Arthritis Res Ther*, 2018.
757 **20**(1): p. 193.
758 29. Oke, V., et al., High levels of circulating interferons type I, type II and type III associate with
759 distinct clinical features of active systemic lupus erythematosus. *Arthritis Res Ther*, 2019.
760 **21**(1): p. 107.
761 30. Pickering, M.C. and M.J. Walport, Links between complement abnormalities and systemic
762 lupus erythematosus. *Rheumatology (Oxford)*, 2000. **39**(2): p. 133-41.
763 31. Perrin, L.H., P.H. Lambert, and P.A. Miescher, Complement breakdown products in plasma
764 from patients with systemic lupus erythematosus and patients with membranoproliferative or
765 other glomerulonephritis. *J Clin Invest*, 1975. **56**(1): p. 165-76.
766 32. Schrager, M.A. and N.F. Rothfield, Clinical significance of serum properdin levels and
767 properdin deposition in the dermal-epidermal junction in systemic lupus erythematosus. *J*
768 *Clin Invest*, 1976. **57**(1): p. 212-21.
769 33. Rother, E., et al., Complement split product C3d as an indicator of disease activity in systemic
770 lupus erythematosus. *Clin Rheumatol*, 1993. **12**(1): p. 31-5.
771 34. Kao, A.H., et al., Erythrocyte C3d and C4d for monitoring disease activity in systemic lupus
772 erythematosus. *Arthritis Rheum*, 2010. **62**(3): p. 837-44.
773 35. Santer, D.M., et al., C1q deficiency leads to the defective suppression of IFN-alpha in
774 response to nucleoprotein containing immune complexes. *J Immunol*, 2010. **185**(8): p. 4738-
775 49.
776 36. Cunninghame Graham, D.S., et al., Polymorphism at the TNF superfamily gene TNFSF4
777 confers susceptibility to systemic lupus erythematosus. *Nat Genet*, 2008. **40**(1): p. 83-9.
778 37. Cortini, A., et al., B cell OX40L supports T follicular helper cell development and contributes
779 to SLE pathogenesis. *Ann Rheum Dis*, 2017. **76**(12): p. 2095-2103.
780 38. Sands, B.E., et al., Phase 2 Trial of Anti-TL1A Monoclonal Antibody Tulisokibart for Ulcerative
781 Colitis. *N Engl J Med*, 2024. **391**(12): p. 1119-1129.
782 39. Glocker, E.O., et al., Inflammatory bowel disease and mutations affecting the interleukin-10
783 receptor. *N Engl J Med*, 2009. **361**(21): p. 2033-45.
784 40. Kirou, K.A., et al., Activation of the interferon-alpha pathway identifies a subgroup of systemic
785 lupus erythematosus patients with distinct serologic features and active disease. *Arthritis*
786 *Rheum*, 2005. **52**(5): p. 1491-503.
787 41. Zhuang, H., et al., Association of anti-nucleoprotein autoantibodies with upregulation of Type
788 I interferon-inducible gene transcripts and dendritic cell maturation in systemic lupus
789 erythematosus. *Clin Immunol*, 2005. **117**(3): p. 238-50.
790 42. Zhang, X., et al., Human intracellular ISG15 prevents interferon-alpha/beta over-amplification
791 and auto-inflammation. *Nature*, 2015. **517**(7532): p. 89-93.
792 43. Care, M.A., et al., Network Analysis Identifies Proinflammatory Plasma Cell Polarization for
793 Secretion of ISG15 in Human Autoimmunity. *J Immunol*, 2016. **197**(4): p. 1447-59.
794 44. Peters, A.L., L.L. Stunz, and G.A. Bishop, CD40 and autoimmunity: the dark side of a great
795 activator. *Semin Immunol*, 2009. **21**(5): p. 293-300.
796 45. Goules, A., et al., Elevated levels of soluble CD40 ligand (sCD40L) in serum of patients with
797 systemic autoimmune diseases. *J Autoimmun*, 2006. **26**(3): p. 165-71.

46. Mohan, C., et al., Interaction between CD40 and its ligand gp39 in the development of murine lupus nephritis. *J Immunol*, 1995. **154**(3): p. 1470-80.
47. Early, G.S., W. Zhao, and C.M. Burns, Anti-CD40 ligand antibody treatment prevents the development of lupus-like nephritis in a subset of New Zealand black x New Zealand white mice. Response correlates with the absence of an anti-antibody response. *J Immunol*, 1996. **157**(7): p. 3159-64.
48. Boumpas, D.T., et al., A short course of BG9588 (anti-CD40 ligand antibody) improves serologic activity and decreases hematuria in patients with proliferative lupus glomerulonephritis. *Arthritis Rheum*, 2003. **48**(3): p. 719-27.
49. Jayne, D.R., et al., Clinical and Biomarker Responses to BI 655064, an Antagonistic Anti-CD40 Antibody, in Patients With Active Lupus Nephritis: A Randomized, Double-Blind, Placebo-Controlled, Phase II Trial. *Arthritis Rheumatol*, 2023. **75**(11): p. 1983-1993.
50. Stohl, W. and D.M. Hilbert, The discovery and development of belimumab: the anti-BLyS-lupus connection. *Nat Biotechnol*, 2012. **30**(1): p. 69-77.
51. Gladman, D.D., D. Ibanez, and M.B. Urowitz, Systemic lupus erythematosus disease activity index 2000. *J Rheumatol*, 2002. **29**(2): p. 288-91.
52. van Vollenhoven, R.F., et al., 2021 DORIS definition of remission in SLE: final recommendations from an international task force. *Lupus Sci Med*, 2021. **8**(1).
53. Bakdash, J.Z. and L.R. Marusich, Repeated Measures Correlation. *Front Psychol*, 2017. **8**: p. 456.
54. Korotkevich, H., et al., Fast gene set enrichment analysis. *bioRxiv*, 2021.
55. Liberzon, A., et al., The Molecular Signatures Database (MSigDB) hallmark gene set collection. *Cell Syst*, 2015. **1**(6): p. 417-425.
56. Kolde, R., et al., Robust rank aggregation for gene list integration and meta-analysis. *Bioinformatics*, 2012. **28**(4): p. 573-80.
57. Yu, G. and Q.Y. He, ReactomePA: an R/Bioconductor package for reactome pathway analysis and visualization. *Mol Biosyst*, 2016. **12**(2): p. 477-9.
58. Langfelder, P. and S. Horvath, WGCNA: an R package for weighted correlation network analysis. *BMC Bioinformatics*, 2008. **9**: p. 559.
59. Shannon, P., et al., Cytoscape: a software environment for integrated models of biomolecular interaction networks. *Genome Res*, 2003. **13**(11): p. 2498-504.
60. Buang, N., et al., Type I interferons affect the metabolic fitness of CD8(+) T cells from patients with systemic lupus erythematosus. *Nat Commun*, 2021. **12**(1): p. 1980.